Molecular Cell
Article

NEMO Ensures Signaling Specificity of the Pleiotropic IKKβ by Directing Its Kinase Activity toward IκBα

Bärbel Schröfelbauer,[1,2] Smarajit Polley,[2] Marcelo Behar,[1,2] Gourisankar Ghosh,[2] and Alexander Hoffmann[1,2,*]
[1]Signaling Systems Laboratory
[2]Department of Chemistry and Biochemistry
University of California, San Diego, 9500 Gilman Drive, La Jolla, CA 92093-0375, USA
*Correspondence: ahoffmann@ucsd.edu
DOI 10.1016/j.molcel.2012.04.020

SUMMARY

Besides activating NFκB by phosphorylating IκBs, IKKα/IKKβ kinases are also involved in regulating metabolic insulin signaling, the mTOR pathway, Wnt signaling, and autophagy. How IKKβ enzymatic activity is targeted to stimulus-specific substrates has remained unclear. We show here that NEMO, known to be essential for IKKβ activation by inflammatory stimuli, is also a specificity factor that directs IKKβ activity toward IκBα. Physical interaction and functional competition studies with mutant NEMO and IκB proteins indicate that NEMO functions as a scaffold to recruit IκBα to IKKβ. Interestingly, expression of NEMO mutants that allow for IKKβ activation by the cytokine IL-1, but fail to recruit IκBs, results in hyperphosphorylation of alternative IKKβ substrates. Furthermore IKK's function in autophagy, which is independent of NFκB, is significantly enhanced without NEMO as IκB scaffold. Our work establishes a role for scaffolds such as NEMO in determining stimulus-specific signal transduction via the pleiotropic signaling hub IKK.

INTRODUCTION

Reliable cellular signal transduction depends on the specificity of kinases. Unlike some metabolic enzymes, in which the catalytic site may show great specificity for particular small molecule substrates, protein kinases require specificity domains. When such specificity domains are encoded by distinct specificity factors, the kinase activity can in principle be directed to alternate specific substrates, allowing for functional pleiotropy (Bhattacharyya et al., 2006; Ubersax and Ferrell, 2007). One may distinguish between catalytic (or "allosteric") specificity factors, that alter the intrinsic catalytic activity of the kinase toward a specific substrate, and scaffold (or "tethering") specificity factors, that enhance otherwise weak interactions between substrate and kinase (Burack and Shaw, 2000). Whereas the c-Jun N-terminal kinase (JNK)-interacting protein (JIP1), the JNK/SAPK-activating protein 1 (JSAP1), and the kinase suppressor of Ras (KSR) are thought to be in the former category, the axin scaffolding proteins target the pleiotropic kinases GSK3 and CK1 to the β-catenin pathway (Burack and Shaw, 2000; Wu and Pan, 2010; Amit et al., 2002), and the Ste5 scaffold directs the specificity of yeast MAPK signaling (Schwartz and Madhani, 2004; van Drogen and Peter, 2002). Indeed, shuffling of binding pockets of Ste5 by site-directed mutagenesis enables redirection of signaling specificity (Dueber et al., 2003). Thus, multivalent scaffold proteins may not only direct kinase substrate specificity but also ensure signaling specificity of a pleiotropic kinase by coordinating upstream and downstream signaling axes.

The IκB kinase (IKK) complex is ubiquitously expressed and functionally pleiotropic (Hayden and Ghosh, 2008; Scheidereit, 2006). Its major catalytic component, IKKβ (also known as IKK2), was purified as the IκB kinase that controls nuclear translocation of NFκB to initiate proinflammatory gene transcription by phosphorylating the canonical IκBs, IκBα, IκBβ, and IκBε (Hayden and Ghosh, 2008; Hoffmann and Baltimore, 2006; Scheidereit, 2006). However, recent literature suggests that IKKβ also plays critical roles in many other biological processes, including autophagy, insulin signaling, and DNA damage responses, by targeting diverse alternative cellular substrates for phosphorylation (Figure 1A) (reviewed in Chariot [2009] and Scheidereit [2006]).

The large number of substrates, and the diverse biological functions regulated by their phosphorylation raise the question of whether IKKβ enzymatic activity may be targeted to distinct substrates. To ensure fidelity as a signal transducer of diverse signals, one would expect the activation of the kinase by upstream pathways to be coordinated with downstream substrate selection.

RESULTS

Constitutively Active IKKβ Requires NEMO for NFκB Activation

In response to the inflammatory cytokine IL-1 IKKβ rapidly phosphorylates S32/36 of IκBα, thereby triggering its ubiquitin-dependent proteasomal degradation, while phosphorylation of the NFκB subunit p65 occurs with delayed kinetics (Figures 1B and S1A). However, using purified, constitutively active IKKβ

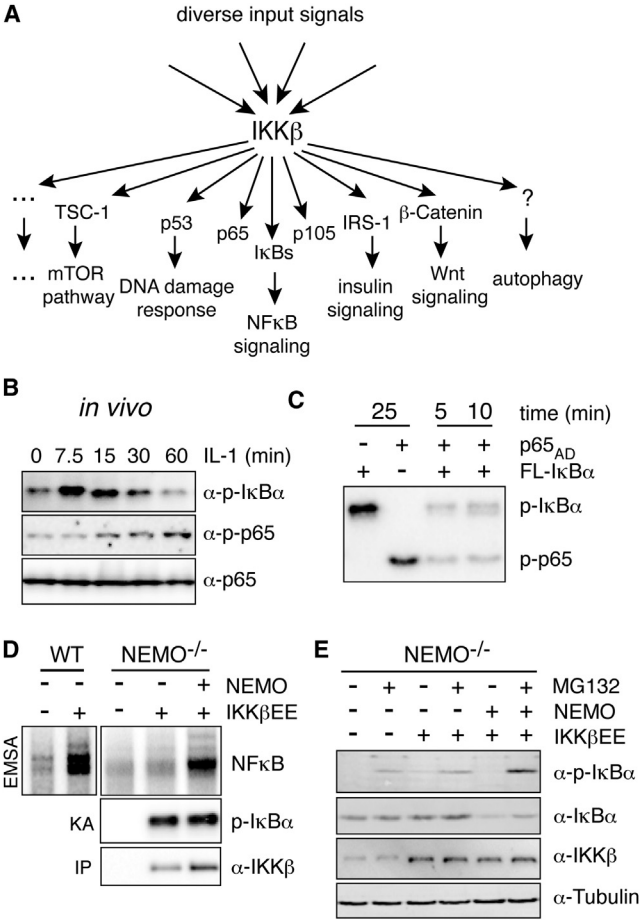

Figure 1. Constitutively Active IKKβ Is Not Sufficient for NFκB Activation, but Requires NEMO

(A) IKK is a pleiotropic transducer capable of phosphorylating many substrates involved in different biological functions. IKKβ phosphorylates the tumor suppressor p53 at S362 and S366 to regulate its stability (Xia et al., 2009), the insulin Receptor (IR) substrate 1 (IRS-1) at S307 resulting in the termination of metabolic insulin signaling (Gao et al., 2002), the tumor suppressor Tuberous sclerosis 1 (TSC1) at S487 and S511 to activate the mTOR pathway, enhance angiogenesis and tumor development (Lee et al., 2007), β-catenin, a key molecule in Wnt signaling, as well as FOXO3a which acts downstream of growth factor signaling (PI3K/Akt) (Lamberti et al., 2001). Induction of autophagy depends on IKKβ kinase activity; the relevant substrates remain to be identified (Comb et al., 2011; Criollo et al., 2010).

(B) Phosphorylation of IκBα (S32/36) and p65 (S536) was measured in fibroblasts upon stimulation with 1 ng/ml IL-1β.

(C) In vitro activity of constitutively active HA-IKKβEE purified from transfected 293T cells was measured using FL-IκBα or the activation domain of p65 ($p65_{AD}$) alone (25 min incubation) or mixed together. Time indicates kinase reaction time.

(D) Steady-state NFκB activity was measured by EMSA in NEMO-deficient cells supplemented with indicated constructs, and IKK kinase activity was determined in an in vitro kinase reaction using FL-IκBα as substrate upon immunoprecipitation of IKKβ with an HA antibody.

(E) Western blot analysis of IκBα phosphorylation and steady-state expression levels in indicated cells with or without MG132 treatment. See also Figure S1.

(HA- IKKβEE) in an in vitro kinase assay, we find high phosphorylation of both IκBα and p65 proteins with no preference for IκBα (Figure 1C) suggesting that in vivo IKKβ's preference for IκB phosphorylation is regulated by additional factors. In vivo, IKKβ activation in response to inflammatory cytokine and pathogen-associated molecular patterns (PAMPs) stimulation requires NEMO, which connects the kinase complex to ubiquitin chains emanating from receptor-associated signaling complexes (Israël, 2010). To test whether NEMO may also be determining the target specificity of the catalytic enzyme, we used a constitutively active form of IKKβ generated through mutation of the critical activation loop serines 177 and 181 to phosphomimetic glutamates (IKKβEE). Retroviral transduction of wild-type fibroblasts with IKKβEE resulted in the expected increase in steady-state NFκB activity, but similar expression of IKKβEE in NEMO-deficient cells had only a modest effect (Figure 1D). However, reconstitution with retrovirally expressed NEMO restored the strong NFκB DNA binding activity. Strikingly, in vitro kinase assays with immunoprecipitated IKK using either FL-IκBα (Figure 1D) or GST-$IκBα_{1-54}$ (Figure S1B) as substrate showed that NEMO did not alter the catalytic IKK activity in these cells, suggesting that it has a specific role in the NFκB activation pathway at a step downstream of its known function in IKK activation. Indeed, we found that IKKβEE caused only weak IκBα phosphorylation and degradation in unstimulated NEMO-deficient cells, unless NEMO was reconstituted (Figure 1E). Taken together these data indicate that intrinsic substrate specificity of IKKβ is not sufficient for efficient IκB phosphorylation, but that NEMO plays a role in targeting IKK activity toward the IκB-NFκB signaling module.

The ZF of NEMO Is Required for Efficient Phosphorylation of IκBα

NEMO's N-terminal region interacts with IKKβ, and the central CoZi-region allows for dimerization and binding to linear and K63 polyubiquitin chains, connecting IKK to inflammatory receptor pathways (Figure 2A) (Israël, 2010). A frameshift mutation that completely removes NEMO's C-terminal Zinc finger (ZF) causes incontinentia pigmenti; its molecular function however remains unclear (Makris et al., 2002). While it is critical for NFκB activation triggered by genotoxic stress (Huang et al., 2002), its role in inflammation-induced NFκB activation is cell- and stimulus-specific. Disruption of the ZF was found to prevent TNF- but not IL-1β-induced NFκB activation in MEFs (Makris et al., 2002). A complete defect in cytokine-induced NFκB activation was observed in human T cells expressing human C417R NEMO (corresponding to C410R in mouse NEMO) (Yang et al., 2004), while NFκB activation by LPS was normal in mouse B cells expressing this mutant (Huang et al., 2002). More recently the ZF has been implicated in enhancing the affinity of NEMO for binding to K63 linked polyubiquitin chains, important for IKK activation by specific stimuli (Laplantine et al., 2009). We examined the possible role of the NEMO ZF on NFκB activation in the context of constitutively active IKKβ. We generated a truncation (ΔC25), a debilitating (C389/393S), and a neutral (M408S) mutant of the ZF domain. Reconstitution of NEMO-deficient cells with these constructs resulted in expression levels comparable to those in wild-type MEFs (Figure S2A). In cells expressing either WT or the M408S NEMO, which does not affect the overall structure of the ZF, strong NFκB activity was detected (Figure 2B), while only modest

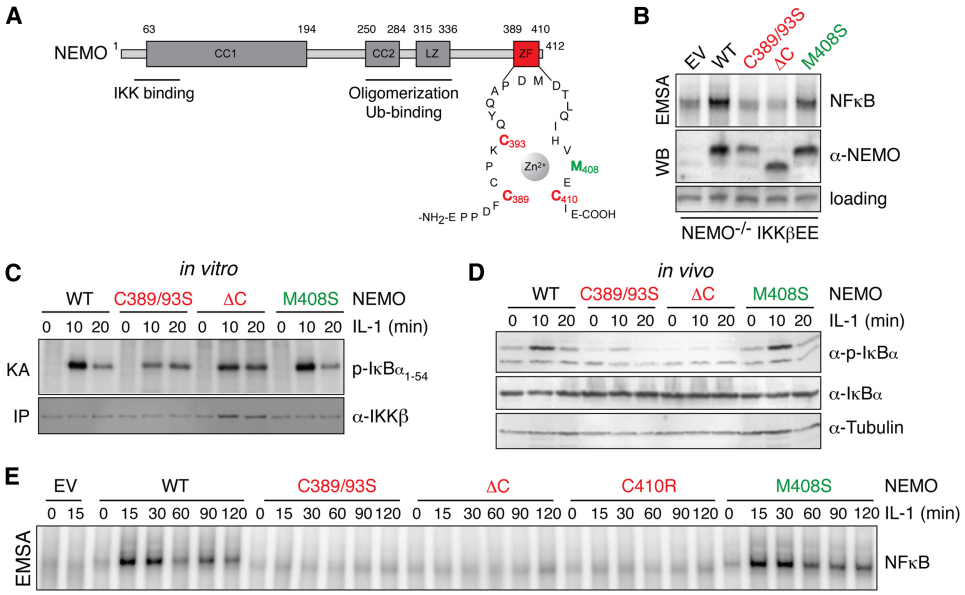

Figure 2. The Zinc-Finger of NEMO Is Dispensable for IKK Activation by IL-1 but Necessary for NFκB DNA Binding Activity

(A) Domain structure of mouse NEMO. NEMO contains two coiled-coil domains (CC1 and CC2), a leucine zipper (LZ) motif, and a zinc finger (ZF). Mutations introduced into the NEMO ZF are highlighted in red and green.

(B) NFκB activity (top) was measured in NEMO-deficient cells expressing IKKβEE and indicated NEMO constructs by EMSA. Expression levels of NEMO are shown below.

(C) NEMO-associated kinase activity was determined in NEMO-deficient cells expressing indicated mutant NEMO in an in vitro IP-kinase assay upon stimulation with IL-1 for indicated times.

(D) Western blot analysis of phosphorylation status and total levels of IκBα upon stimulation with IL-1.

(E) NFκB DNA binding activity of NEMO-deficient cells reconstituted with the indicated mutant NEMO constructs was measured by EMSA upon stimulation with IL-1 (10 ng/ml). See also Figure S2.

nuclear NFκB activity was observed in NEMO-deficient cells. Strikingly, truncating and debilitating the ZF abolished NEMO's ability to reduce IκBα levels (as well as IκBβ and IκBε, Figure S2B) and to enhance NFκB activity in the presence of IKKβEE (Figure 2B). These data suggest that the ZF of NEMO is critical for the active IKK complex to efficiently target IκBs for degradation in vivo, to allow for NFκB activation, even though ZF mutations had no effect on in vitro IKK kinase activity (Figure S2C).

To examine NEMO's role in targeting IKK toward IκBs during inflammatory signaling, we had to identify conditions in which NEMO mutants, defective in IκB targeting, allowed for efficient IKK activation. NEMO-deficient cells reconstituted with NEMO mutants were exposed to TNF, IL-1β, and LPS. In cells expressing WT NEMO and M408S mutant NEMO, all stimuli induced in vitro kinase activity, although kinase activity induced by TNF was attenuated in M408S NEMO-expressing cells (Figures 2C, S2D, and S2E). IL-1β and LPS also induced strong, yet somewhat weaker kinase activity in cells expressing NEMO with a truncated or debilitated ZF (Figures 2C and S2D), though both mutants were defective in supporting TNFα-induced kinase activity (Figure S2E), consistent with data reported by Makris et al. (2002). Thus, the ZF of NEMO appears to be largely dispensable for the activation of the IKK complex by IL-1β and LPS in fibroblasts, reflecting stimulus-specific requirements for IKK activation.

If the ZF were necessary for recruiting the IKK complex to IκBs, a defect in IκBα phosphorylation and degradation and subsequent NFκB activation in cells expressing ZF-mutated NEMO would be anticipated. As expected, in NEMO$^{-/-}$cells expressing WT NEMO or a neutral M408S mutant, phosphorylation and degradation of IκBα were induced by IL-1β (Figure 2D). However, in cells expressing NEMO with a truncated or debilitated ZF, IL-1β stimulation triggered neither IκBα phosphorylation nor degradation. Furthermore, NFκB DNA binding activity induced by IL-1β, LPS, and TNF was defective with ZF mutants while it was strongly activated in WT and M408S-expressing cells (Figures 2E, S2F, and S2G). The reduction in kinase activity measured in cells expressing truncated or C389/93S NEMO could not account for the observed defect in NFκB activation, as similarly low kinase activities in WT cells (elicited by lower stimulus concentrations) allowed for detection of strong NFκB DNA binding ability (Figure S2H). These data are consistent with results obtained with constitutively active IKKβ and further indicate that NEMO does indeed play a role in NFκB activation that is distinct from its function in activating the IKK complex, most likely by facilitating the recruitment of IκBs to the IKK complex.

NEMO Forms a Complex with IKKβ and IκBα

NEMO's apparent role as a specificity factor for IKK may be mediated by allostery altering the catalytic specificity of the enzyme or by functioning as a scaffold tethering IκB substrates toward the catalytic site. Given that in vitro kinase assays did not reveal differences in catalytic activity, we hypothesized that

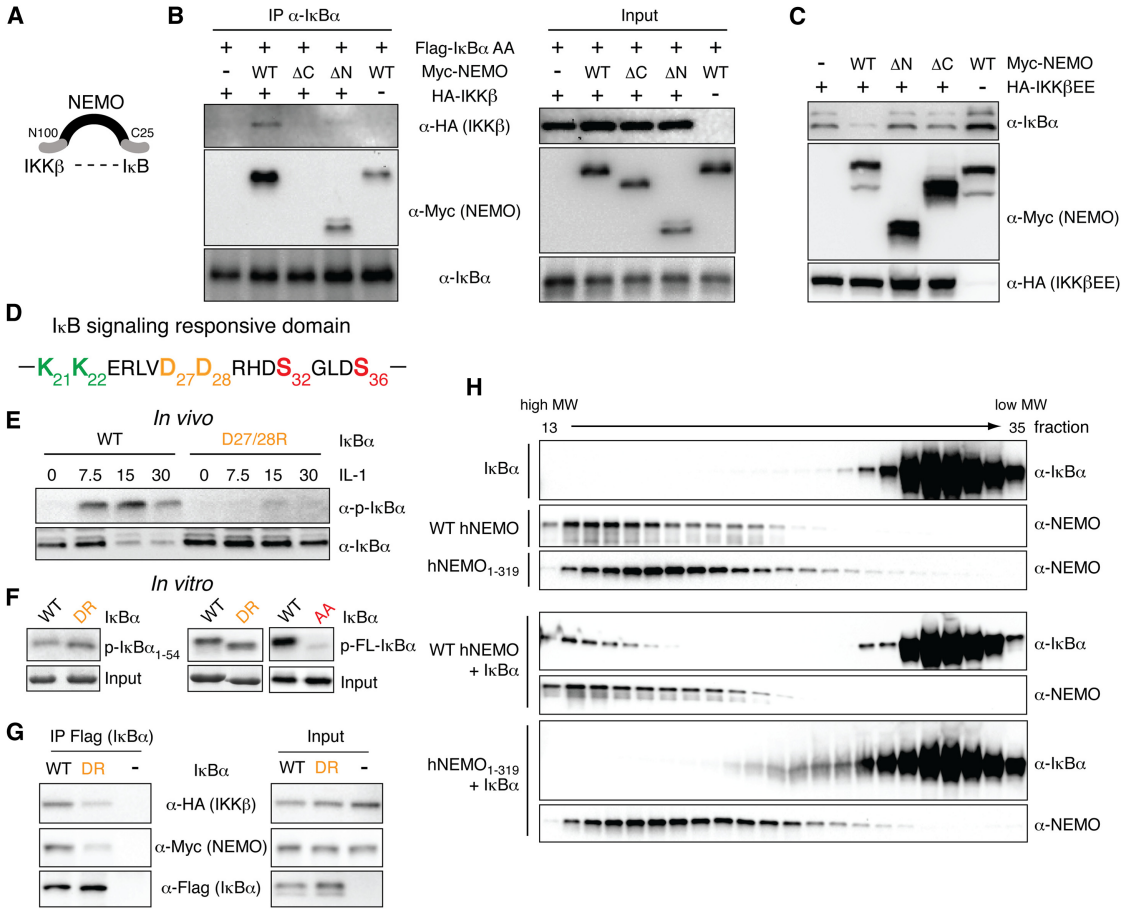

Figure 3. NEMO Forms a Complex with IKKβ and IκBα

(A) Schematic of a possible complex between NEMO, IKKβ, and IκBα. The N-terminal 100 amino acids of NEMO facilitate interaction with IKKβ, while the C-terminal ZF might allow for interaction with IκBα.

(B) NEMO interacts with IκBα via its C terminus. 293T cells were transfected with nondegradable FLAG-IκBα (FLAG-IκBα AA), HA-IKKβ, and WT or mutant Myc-NEMO constructs. Left panel: Complexes were analyzed upon immunoprecipitation of IκBα by western blotting using indicated antibodies. Right panel: Expression levels of inputs were analyzed in parallel.

(C) The NEMO C terminus is required for signaling to IκBα. 293T cells were transfected with small amounts of IKKβEE together with indicated NEMO mutants, and IκBα steady-state levels were analyzed by western blotting.

(D) Amino acid sequence of the IκBα signaling responsive domain. Key amino acids discussed in the text are shown in color.

(E) Phosphorylation and expression of WT and DR mutated IκBα stably expressed in IκBα-deficient cells was analyzed upon stimulation with IL-1 by western blotting. Loading was adjusted to similar IκBα levels.

(F) Phosphorylation of WT or DR mutant IκBα by IKKβEE was analyzed in an in vitro kinase assay using wild-type or DR mutant GST-IκBα$_{1-54}$ (left panel) or FL-IκBα (middle panel) or FL- IκBα with S32/36 mutated to alanine (AA) to control for specificity.

(G) Interaction between WT and DR IκBα with NEMO and IKKβ was analyzed by immunoprecipitation of IκBα with an α-FLAG antibody from 293T cells followed by western blot analysis with indicated antibodies.

(H) Gel filtration of recombinant FL-human IκBα, wild-type, or 1–319 truncated human NEMO. Proteins were mixed at a ratio of 1:1 prior to gel filtration. Fractions 13–35 were analyzed by western blotting. See also Figure S3.

NEMO functions as a recruitment scaffold by enhancing the IKK-IκB interaction through an N-terminal interaction with IKKβ and a C-terminal interaction with IκBα (Figure 3A). To test this hypothesis, IκBα was immunoprecipitated and its interaction with IKKβ and NEMO was analyzed by immunoblotting (Figure 3B). A strong interaction between IκB and IKK could be detected in the presence of WT NEMO, but not in its absence. Deletion of the ZF abolished binding. The interaction was dependent on IKKβ, as the interaction of IκB with WT NEMO was reduced in the absence of IKKβ or when an N-terminally truncated NEMO, which lacks the IKKβ binding site, was used. Comparable results were obtained when NEMO was immunoprecipitated (Figure S3). Together, these data indicate that NEMO interacts with IκBα, that the ZF is required for this interaction, and that the interaction is strengthened in the presence of IKKβ, suggesting the existence of a IκB:IKK:NEMO complex.

In a functional assay, in which steady-state expression of IκBα was analyzed in the presence of small amounts of IKKβEE,

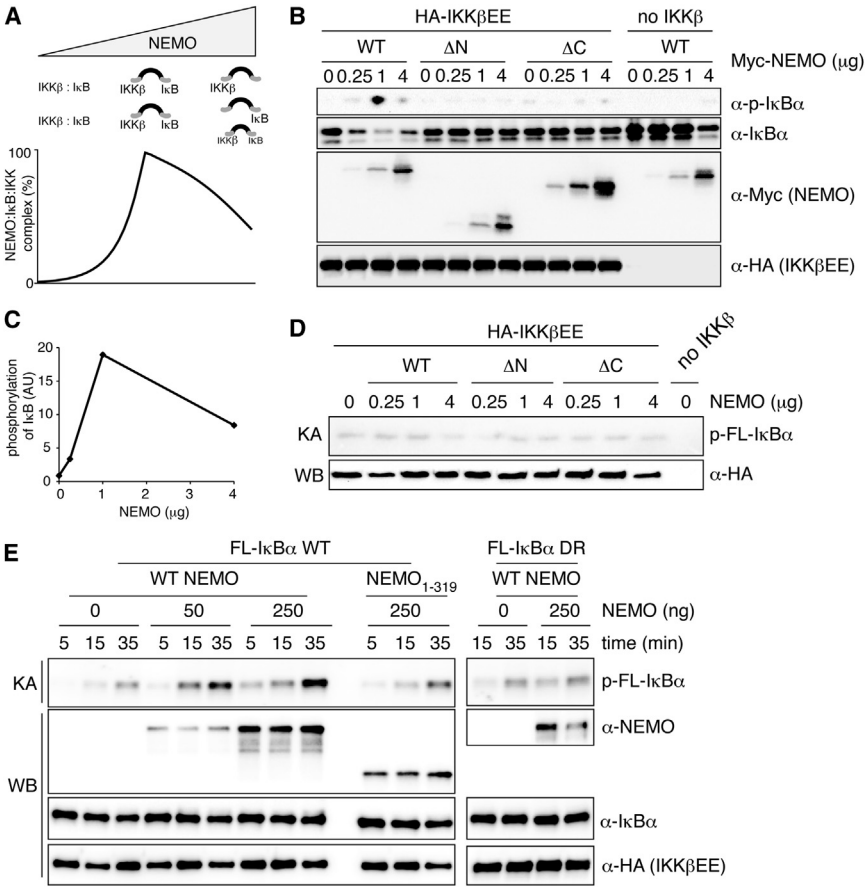

Figure 4. NEMO Functions as a Scaffold In Vivo and In Vitro

(A) Schematic and computational model simulation to illustrate combinatorial inhibition and its consequence on NEMO:IκB:IKK complex formation and IκBα phosphorylation.

(B) 293T cells were transfected with HA-IKKβEE and increasing amounts of WT or mutant NEMO constructs. Levels of phosphorylated and total IκBα were analyzed by western blotting.

(C) Quantification of IκBα phosphorylation in (B). p-IκBα was normalized to total IκBα expression.

(D) In vitro kinase assay from 293T cells transfected with HA-IKKβEE and indicated amounts of WT or mutant NEMO constructs. FL-IκBα was used as substrate.

(E) In vitro kinase assay using HA-IKKβEE purified from transfected 293T cells using 50 ng of full-length wild-type or DR IκBα as substrate in the presence of 10 μg BSA as nonspecific competitor. 50 or 250 ng recombinant human wild-type of 1–319 NEMO were added to the reaction as indicated. Time indicates kinase reaction time. Inputs were analyzed by western blotting in parallel. See also Figure S4.

reduced levels of IκBα could only be detected when WT NEMO was cotransfected, but not when N- and C-terminally truncated NEMO was expressed, further suggesting that NEMO indeed enhances IκBα turnover by means of complex formation with IκBα and IKKβ (Figure 3C).

The N-terminal 54 amino acids of IκBα are known to be sufficient for phosphorylation by IKKβ (Figure 3D) (Wu and Ghosh, 2003). As NEMO appears to be important for targeting IKKβ to IκBα, IκBβ, and IκBε, we hypothesized that a region conserved in canonical IκBs would mediate the interaction with NEMO. Most mutations of conserved residues in IκBα showed no defects in phosphorylation and degradation upon stimulation with IL-1β (data not shown). However, mutation of negatively charged residues D27 and D28 (corresponding to D14 and E15 in IκBβ) to positively charged arginines resulted in a strong reduction of inducible phosphorylation and degradation upon stimulation with IL-1β (Figure 3E), indicating that these amino acids are critical for phosphorylation by IKKβ in cells. IKKβEE-induced phosphorylation of both the full-length and 1–54 IκB D27/28R mutants was comparable with WT IκBα in in vitro kinase assays (Figure 3F), indicating that the consensus phosphorylation site for IKKβ was not disrupted by the mutation. Instead, the in vivo defect in phosphorylation may be due to impaired recruitment by NEMO as the D27/28R IκBα mutation weakened IκBα's interaction with NEMO and IKK2 (Figure 3G). Together, these data indicate that in cells, NEMO forms a complex with IκBα and IKKβ and that amino acids D27 and D28 in the N terminus of IκBα are critical for complex formation.

To test the interaction between NEMO and IκBα more directly, we produced highly purified recombinant, bacterially expressed NEMO and IκBα and performed gel filtration analysis. As shown in Figure 3H, free IκBα was detected in the low molecular weight fractions 26–35. In the presence of full-length NEMO IκBα was also present in NEMO-containing high molecular weight fractions (13–18). In contrast, no change in the elution profile of IκBα was detected in the presence of a C-terminal NEMO deletion mutant (lower panel). These data are indicative of a direct interaction between NEMO and IκBα that depends on NEMO's C terminus.

NEMO Functions as a Scaffold for IKKβ

A hallmark of scaffold proteins is a nonmonotonic dose response curve: increasing amounts of scaffold allow for increased complex formation, but when the scaffold concentration exceeds that of the kinase or substrate whose interaction it coordinates, then the excess will inhibit the formation of the full complex, by instead favoring the formation of many incomplete subcomplexes, an effect referred to as "combinatorial inhibition" (Ferrell, 2000; Levchenko et al., 2000). Accordingly, computational simulations of a mathematical model for the formation of the IκB-NEMO-IKK complex (Supplemental Experimental Procedures) showed increased complex formation when NEMO amounts are increased within a substoichiometric regime, but reduced functional complexes within a higher regime (Figure 4A). To test this experimentally, we transfected 293T cells with increasing amounts of NEMO and limiting amounts of IKKβEE. Expression of small to intermediate amounts of NEMO

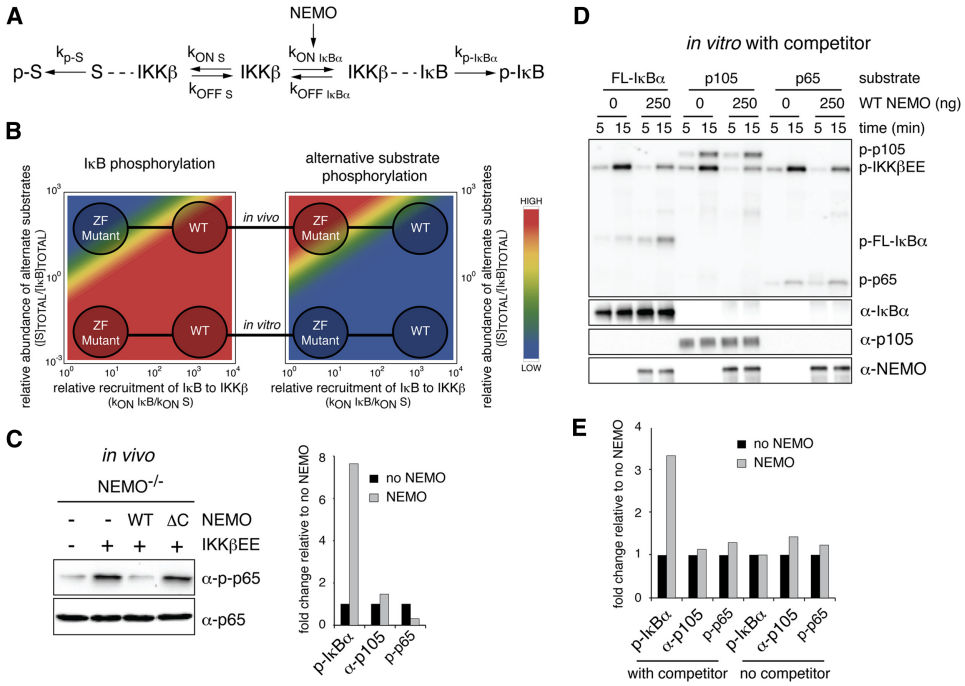

Figure 5. Substrate Competition between IκBα, p65, and p105

(A) A model for competitive complex formation between IKK and IκB or alternative substrates. The presence of NEMO favors IKK:IκB complex formation, here modeled as NEMO-dependent increase of k_{ON}IκB.

(B) In silico model for IκB phosphorylation. Fraction of IKK bound to IκB and alternative substrate S (right and left, respectively) as a function of the NEMO-induced stabilization of the IKK-IκB complex (x axis) and the relative concentration of alternative substrate S (y axis). The "in vitro" region is characterized by a very low ratio of S to IκB in contrast to the "in vivo" situation, in which large amounts of alternative substrates S might be present.

(C) NEMO-deficient cells were stably reconstituted with indicated vectors and phosphorylation of p65 at S536 was analyzed by western blotting. Quantification of steady-state phosphorylation of IκBα (Figure 1E), p105 (Figure S5A) and p65 (left panel). Phosphorylation signals were normalized to total protein and phosphorylation in the absence of NEMO was set to 1.

(D) In vitro kinase assay of HA-IKKβEE using 50 ng of FL-IκBα, FL-p105, or p65AD as substrate in the presence of 10 μg BSA. Where indicated, 250 ng recombinant WT NEMO were added. Inputs were analyzed by western blotting.

(E) Quantification of phosphorylation of IκBα, p105, and p65 from kinase assays with competitor and limited substrate (D) and without competitor and access substrate (Figure S5C) after a 15 min kinase reaction. Phosphorylation in the absence of NEMO was set to 1. See also Figure S5.

led to a dose-dependent increase of IκB phosphorylation and reduced levels of total IκBα expression (Figure 4B and quantification Figure 4C) caused by intrinsic IKKβEE activity. Strikingly, high overexpression resulted in reduced phosphorylation of IκBα and increased IκBα levels. Expression of NEMO mutants that only interacted with either IKKβ (NEMO ΔC25) or IκBα (NEMO ΔN) had no effect. The kinase activity, assayed in vitro, remained unchanged throughout all NEMO expression levels (Figures 4D and S4). Thus, in the context of physical interactions delineated in Figures 3B–3H, the functional characteristics described in Figures 4A and 4B support the conclusion that NEMO functions as a specificity scaffold that recruits classical IκBs to IKK.

Throughout these studies of NEMO's role as a specificity factor in vivo, we failed to observe such a function in vitro. We considered the explanation that the substrate availability/concentration in cells is lower than in in vitro kinase assay reaction conditions, in which substrate is supplied in excess to ensure sensitivity and linear dose responses. To test this hypothesis we attempted to mimic in vivo conditions by performing the kinase reaction in the presence of high concentrations of nonspecific competitor protein (BSA) and limiting concentrations of substrate. Using these conditions, IκBα phosphorylation was stronger and occurred with faster kinetics in the presence than in the absence of NEMO (Figure 4E). In contrast, ZF-deleted NEMO failed to enhance IκBα phosphorylation. Similarly NEMO had no effect on phosphorylation of IκBα DR, which is phosphorylation defective in vivo. These data further support the notion that NEMO acts as a scaffold for IKKβ likely by enhancing the local concentration of IκB to allow for its more efficient phosphorylation.

NEMO Directs IKKβ Activity Away from Alternative Substrates

IKKβ is a pleiotropic kinase that is known to phosphorylate numerous alternative substrates in vivo, in addition to IκBα. To analyze the potential effect of the scaffolding function of NEMO in this in vivo scenario we constructed an in silico model for IκB phosphorylation, in which IKKβ can bind to and phosphorylate IκBs or alternative substrates (Figure 5A). Akin to our experimental results (Figure 4E), model simulations suggested

that in the absence of alternative substrates (i.e., in vitro) the ZF-dependent NEMO scaffold function would have little effect on phosphorylation of IκB, while in their presence (i.e., in vivo), efficient phosphorylation of IκB may only occur in the presence of WT but not ZF mutant NEMO (Figure 5B, left panel). In contrast, NEMO's scaffolding function was predicted to restrict the phosphorylation of alternate substrates with the ZF mutant NEMO leading to the hyperphosphorylation of alternative IKKβ substrates (Figure 5B, right panel).

To test this prediction experimentally, we analyzed steady-state phosphorylation of RelA/p65 Ser536, a well-established alternative target of IKKβ. Only low levels of p65 were phosphorylated in NEMO-deficient cells, but IKKβEE expression greatly enhanced phosphorylation levels (Figure 5C). Strikingly, expression of WT NEMO resulted in a strong reduction of phosphorylated p65, while ZF-mutated NEMO showed similar p-p65 levels to the parental NEMO-deficient IKKβEE cells, indicating that in contrast to IκBα, p65 is a NEMO-independent substrate. Indeed, in kinase assays performed in the presence of competitor protein and limiting amounts of substrate to reflect in vivo conditions, NEMO had no effect on the phosphorylation of p65 or p105, while IκBα phosphorylation was strongly enhanced by the addition of NEMO (Figures 5D and 5E). In contrast, without competitor, phosphorylation of IκBα, p65, and p105 was unaffected by NEMO (Figures 5E and S5C). These data not only demonstrate that NEMO does not affect IKKβ kinase activity per se, but that it specifically channels IKKβ kinase activity to IκBα in conditions of low substrate abundance.

Next we asked whether we could observe similar substrate competition in the context of stimulated cells. As expected, IL-1β stimulation rapidly induced IκBα phosphorylation in NEMO-deficient cells reconstituted with WT NEMO, (Figure 6A). No IκBα phosphorylation was detectable in the presence of ZF mutant NEMO but instead alternative IKKβ substrates, p65 and p105, were strongly phosphorylated. Similar results were obtained upon stimulation with LPS (Figure S6A). Phosphorylation of p65 and p105 was indeed caused by IKKβ, as treatment with an IKKβ-specific inhibitor abolished phosphorylation (Figure S6B). Despite hyperphosphorylation of p65 and p105 we did not detect measurable levels of NFκB activity (Figure 2E and data not shown). These data confirm that NEMO not only enhances phosphorylation of IκBs, but also restricts the phosphorylation of alternative substrates.

We next addressed the implicit hypothesis that IκB and alternative substrates are effectively competing in vivo for limited enzyme activity. Using cells that lack the IκB substrates ($i\kappa b\alpha^{-/-}\beta^{-/-}\varepsilon^{-/-}$), phosphorylation of both p65 and p105 was strongly induced as early as 5 min post-IL-1β stimulation, while it was barely induced in WT cells (Figure 6B). These data suggest that NEMO's role as a specificity factor is dependent on the availability of IκB substrates, further supporting a role of NEMO in acting as a scaffold/tethering factor to direct IKK's activity specifically to IκBs.

Recent studies have shown that IκBα phosphorylation and degradation are not required for IKKβ-induced autophagy, suggesting the involvement of alternative IKKβ substrates (Comb et al., 2011; Criollo et al., 2010). Our model of NEMO as a specificity factor for IκBs that restricts the phosphorylation of alternative IKKβ substrates would predict that autophagy may be hyperactivated in cells that express ZF-debilitated NEMO. Indeed, when ZF-deleted NEMO was expressed along with IKKβEE, the number of cells that stained positive for the autophagy marker LC3 was significantly enhanced over that of WT NEMO controls (Figure 6C). Concomitantly, phosphorylation of p70S6K, a marker for mTOR activity, was strongly reduced, while the upstream AMPK was hyperphosphorylated in cells expressing the ZF mutant NEMO (Figure 6D), indicating that the signaling required for the induction of autophagy is hyperactivated by constitutively active IKKβ when NEMOs IκB targeting function is lost. Similarly, starvation increased the number of LC3 positive cells harboring a ZF-deleted NEMO (Figure 6E), despite comparable levels of NEMO-associated IKK kinase activity (Figure S6C). These data further show that autophagy is hyperactivated when IKKβ loses its ability to phosphorylate IκBs, but instead hyperphosphorylates alternative substrates.

DISCUSSION

We have presented several lines of evidence that NEMO plays an essential role in targeting IKK to the IκB-NFκB signaling module. Previous studies focused on NEMO's essential role in the activation of IKK via its ability to bind ubiquitin chains, which are a hallmark of inflammatory signaling by receptors of the TNFR and TLR/IL1R superfamilies. Using a constitutively active IKK variant (Figure 1) and identifying a specific mutation in NEMO (Figure 2), we were able to distinguish between these two essential functions in activation and targeting. Physical interaction studies indicated that IKK-IκB interactions are enhanced by NEMO, which interacts not only with IKK through its N terminus (May et al., 2000; Mercurio et al., 1999) but may also form a stable complex with IκBα via its C terminus (Figure 3). Using combined in silico kinetic modeling and in vivo experimental analysis we showed that the dose-response characteristics of NEMO are indeed consistent with bivalent interactions (Figure 4) that support a scaffolding model for NEMO. Consistent with such a model, NEMO enhances IκB phosphorylation in cells, and in in vitro conditions in which alternative substrates are abundant (Figure 5). NEMO reduces alternate substrate phosphorylation (Figure 6) and channels IKK activity specifically to IκBs; it therefore not only sensitizes the inflammatory pathway but may also increase its responsiveness to transient and dynamically regulated IKK signals (Cheong et al., 2006; Werner et al., 2005).

NFκB activation occurs over a wide dynamic range. In the cyclin-dependent kinase system, alternative substrates are thought to function as competitive inhibitors for specific phosphorylation (Kim and Ferrell, 2007). The resulting ultrasensitivity renders the pathway insensitive to weak signals and responsive only to high levels of stimulus. The role of NEMO may thus be particularly important at low levels of stimulus, as it counteracts the ultrasensitivity brought by an abundance of alternative substrates. However, when IKK is highly activated, NEMO's scaffolding function may be less critical. This may in part explain why Huang et al. (2002) did not observe a strong defect in NFκB activation in a ZF mutant B cell line in response to high doses of LPS.

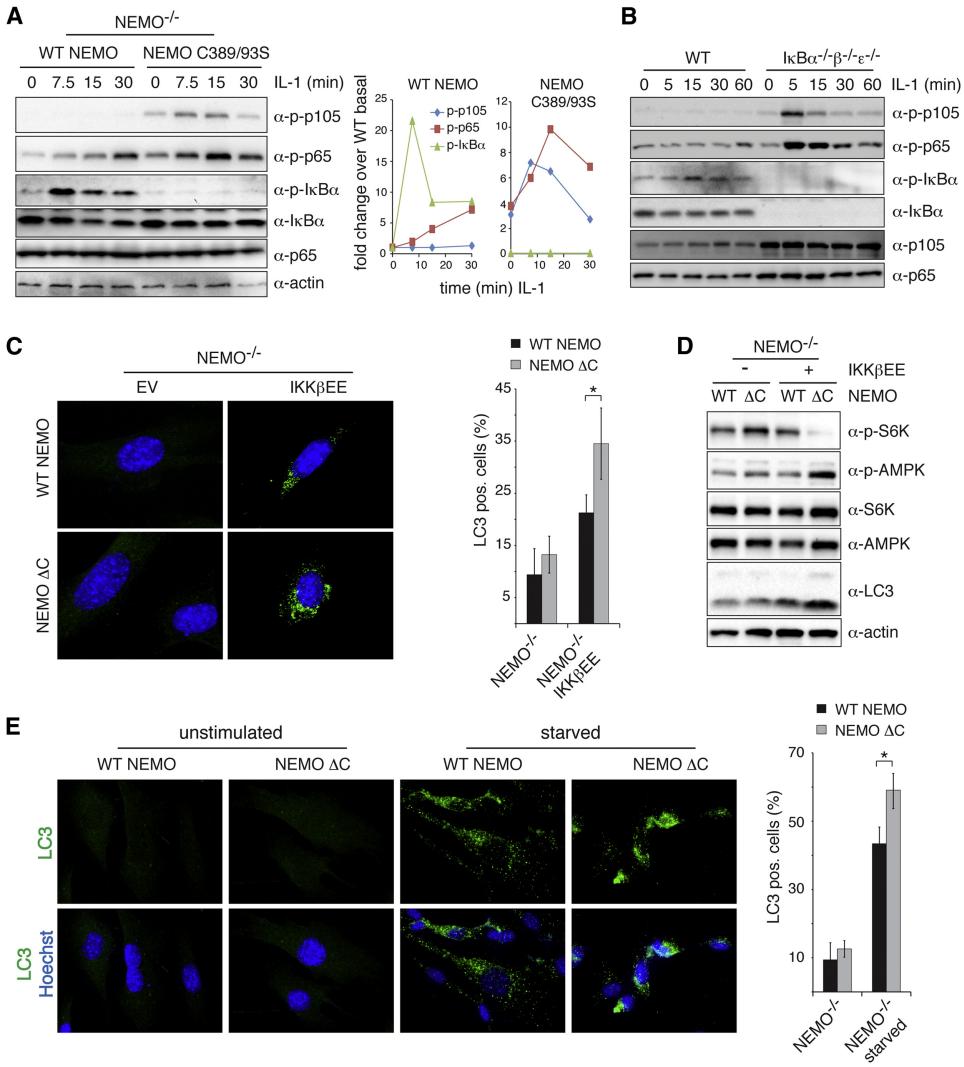

Figure 6. In the Absence of NEMO Scaffolding, IKKβ Hyperphosphorylates Alternative Substrates and Hyperactivates Autophagy

(A) Phosphorylation of p105 (S933), p65 (S536), and IκBα (S32) was measured in NEMO-deficient cells reconstituted with WT or C389/93S mutant NEMO upon stimulation with IL-1. The quantification of this blot is shown on the right.

(B) WT MEFs and IκBα$^{-/-}$β$^{-/-}$ε$^{-/-}$ cells were stimulated with IL-1 and phosphorylation of p105, p65, and IκBα was analyzed by western blotting.

(C) Hyperactivation of NFκB-independent IKKβ-induced autophagy. NEMO-deficient cells stably expressing constitutively active IKKβ and WT or ZF deleted NEMO were stained for LC3 and Hoechst and analyzed by immunofluorescence microscopy. Representative images are shown. Quantification of LC3-positive cells is shown on the right (% cells with LC3 puncta, mean ± SD, n > 150 cells, *p < 0.05).

(D) Western blot analysis of phosphorylated S6K (T389) and AMPKα (T172) in NEMO-deficient cells stably expressing IKKβEE and indicated NEMO construct.

(E) NEMO-deficient cells reconstituted with WT or mutant NEMO were starved with HBSS for 1 hr prior to immunofluorescence staining and analysis. The quantification of LC3-positive cells is shown on the right (% cells with LC3 puncta, mean ± SD, n > 150 cells, *p < 0.05). See also Figure S6.

We show a direct interaction between recombinant purified NEMO and IκBα (Figure 3H). Our coimmunoprecipitation experiments suggest that the NEMO-IκBα interaction is strengthened by IKKβ (Figure 3B), suggesting a stable ternary complex in which the N terminus of NEMO binds to IKK while its C terminus facilitates interaction with IκBα, and IKKβ itself interacts with the C terminus of IκBα through its ULD-SDD domains (Xu et al., 2011). Interestingly, this interaction appears to be important for IKK's specificity. Our data suggest that the N-terminal aspartic acids D27/28 in IκBα are also critical for the efficient phosphorylation of IκBα on S32/36 in vivo, while its ability to be phosphorylated by IKKβ remains intact in vitro. Whether NEMO directly interacts with the IκBα N terminus or whether the N-terminal aspartic acids are participating in binding to IKK to form the functional ternary complex remains to be determined. However, our data support the function of NEMO as a scaffold that enhances the local concentration of IκBα to allow for its specific and rapid phosphorylation.

Our work not only adds to our understanding of NEMO's biological function, it also provides a framework for understanding

IKK as a pleiotropic signal transducer that is involved in numerous biological processes and is capable of stimulus-specific phosphorylation of specific substrates. Although IKK's name suggests specificity for IκB phosphorylation, it is NEMO that determines its substrate specificity and function within the inflammatory pathway. Akin to how the yeast MAPK Ste11p mediates distinct signaling axes responsive to mating pheromone or hyperosmolarity depending on its association with scaffold proteins Ste5p or Pbs2p respectively (Engström et al., 2010; Schwartz and Madhani, 2004; van Drogen and Peter, 2002), NEMO defines the inflammatory signaling axis mediated by IKK, owing to its multivalent interactions with ubiquitin chains, IKK, and IκB. We would expect that other scaffolds might be identified for IKK's alternate functions in autophagy or insulin signaling. Such scaffolds may either be similarly multivalent, capable of replacing NEMO and thus insulating the pathway from inflammatory signaling, or they may be bivalent to function with NEMO to connect IKK to other upstream activation pathways or target IKK to other downstream substrates. The latter scenarios would provide for crosstalk with the inflammatory signaling axis, which may underlie the pleiotropic functions of inflammation itself. On a related note, it is not known whether the IKK-interacting proteins RAP1 or ELKS, which are essential for phosphorylation of p65 (Teo et al., 2010) or activation by genotoxic stress (Wu et al., 2010), respectively, function with NEMO or in its stead. The use of scaffolds to direct IKK's target specificity constitutes a modular strategy to facilitate signaling specificity while allowing for signaling crosstalk within this regulatory hub.

The ΔC25 NEMO mutant described here resembles NEMO expressed in some patients with incontinentia pigmenti (IP) as a result of a frameshift mutation (Makris et al., 2002). IP is an X-linked genetic disease thought to be caused for the most part by inactivation of NFκB signaling and hypersensitivity of NEMO-deficient cells to TNF-induced apoptosis (Courtois and Israël, 2011). Interestingly, in IP mouse models an increase of inflammatory cytokines including TNF and IL-1β could be observed in the epidermis at the early onset of the disease (Makris et al., 2000; Nenci et al., 2006; Pasparakis et al., 2002). Hyperactivation of autophagy reported here might provide an explanation for this disease phenotype, as autophagy has recently been implicated to positively contribute to the biogenesis and secretion of inflammatory cytokines such as IL-1β (Dupont et al., 2011).

To harness the potential of the pleiotropic IKK signal transducer as a drug target in numerous types of inflammatory diseases, diabetes, and cancers, it is critical to understand how its activity is directed to different signaling axes and cellular functions and the degree to which these are insulated from or connected with each other. The present work identifies NEMO as a key molecule in this systems behavior and provides a framework for future investigations.

EXPERIMENTAL PROCEDURES

Cell Culture and Stimulations

Immortalized NEMO-deficient MEFs were generated via the 3T3 protocol from embryos derived from NEMO$^{-/-}$ mice (Rudolph et al., 2000). IκBα$^{-/-}$β$^{-/-}$ε$^{-/-}$ cells and IκBα$^{-/-}$ cells were described previously (Basak et al., 2007). 3T3 cells were reconstituted by retroviral transduction with WT or mutant pBABE.mNEMO.puro, pBABE. IκBα.puro constructs, and/or with pBABE.IKKβEE.hygro or empty vector controls. Cells were selected with puromycin Hydrochloride (Sigma) and hygromycin B (Invitrogen), respectively, and expression of the stably expressed constructs was verified by western blotting. Cells were stimulated with recombinant murine TNFα (Roche), LPS (Sigma), or murine IL-1β (R&D).

Expression and Purification of Recombinant NEMO and IκBα

His-tagged human recombinant full-length or 1–319 truncated human NEMO was cloned into pET29 expression vector. pET29.hNEMO WT or 1–319 and pET15.IκBα were transformed into BL21 cells. Expression was induced with 0.25 mM IPTG at room temperature, and upon sonication proteins were purified in a buffer containing 50 mM Tris (pH 7.5), 300 mM NaCl, 10% Glycerol, 10 mM Imidazole, 25 μM $ZnSO_4$ (for WT NEMO) using Ni-NTA beads. Proteins were eluted in buffer containing 250 mM Imidazole and dialyzed.

Size Exclusion Chromatography

For size exclusion chromatography individual proteins were mixed with each other at a ratio of 1:1 and incubated at room temperature for 1hr to form complexes prior to size exclusion chromatography. 150 μl of each sample was loaded onto a Superose 6 10/300 GL column (GE Healthcare) pre-equilibrated with 25 mM Tris (pH 7.5), 150 mM NaCl, 5% Glycerol, 2 mM DTT and 40 μM $ZnSO_4$ and resolved at a flow rate of 0.5 ml/min on an AkTA (GE Healthcare) automated liquid chromatography system. Size fractions of 0.5 ml were collected and an equal volume aliquot of each fraction was analyzed by western blotting using relevant antibodies indicated in the respective figures.

Gel-Shift Assay and IKK Kinase Assay

Gel-shift assays were performed as previously described (Basak et al., 2007). Briefly, nuclear extracts were incubated with ^{32}P-labeled 38 bp spanning double-stranded oligonucleotides containing two consensus κB sites at room temperature for 20 min prior to complex separation on a nondenaturing acrylamide gel. Bands were visualized by autoradiography and quantified using ImageQuant software. In vitro IKK kinase assays were performed as described previously (Werner et al., 2005). The IKK complex was immunoprecipitated from cytoplasmic extracts using a NEMO-specific antibody (BD or Santa Cruz Biotechnology) and Protein A-sepharose beads. In NEMO-deficient cells, IKK kinase complexes were precipitated using an IKKα antibody (Santa Cruz Biotechnology) or HA antibody (Covance) to pull down HA-tagged IKKβ. Beads were subjected to in vitro kinase reaction containing ^{32}P-ATP and 1 μg GST-IκBα$_{1-54}$, GST-IκBα$_{1-54}$ D27/28R, full-length wild-type or D27/28R His-IκBα, full-length p105 or GST-p65$_{AD}$ as substrates. For competitor experiments 10 μg BSA and 50 ng of substrate and indicated amounts of recombinant wild-type or 1–319 hNEMO were added to the kinase reaction. Upon incubation at 30°C for indicated time, reactions were stopped by boiling samples in SDS sample buffer. Proteins were resolved by SDS-PAGE and visualized by autoradiography or western blotting.

Coimmunoprecipitation and Western Blotting

For western blot analysis, whole-cell extracts were prepared using RIPA buffer supplemented with PMSF, DTT, and phosphatase inhibitors. Samples were normalized for equal amounts of proteins using a Bradford assay (Biorad). Phospho-specific antibodies to IκBα (S32/36) p65 (S536), p105 (S933), p-AMPK (T172) and AMPK, p-p70 S6 Kinase (T389), and p70 S6 Kinase were from Cell Signaling. For coimmunoprecipitation experiments, 293T cells were transfected with indicated amounts of pcMyc-NEMO, pcFLAG-IκBα, and pcHA-IKKβ or empty vector. Total amounts of DNA used for transfections were normalized with empty vector. Cells were lysed in buffer containing 10 mM HEPES-KOH (pH 7.9), 250 mM NaCl, 1 mM EDTA, 0.5% NP-40, 0.2% Tween 20, 1 mM DTT, 1 mM PMSF, and 10 μM MG132. Lysates were precleared with protein A/G sepharose beads followed by immunoprecipitation with anti-Myc (Roche), anti-HA (Covance) or anti-FLAG (Sigma) antibody for 2 hr. Complexes were collected by addition of 10 μl protein A/G Sepharose for 2 hr followed by extensive washing in lysis buffer at 37°C. Samples were analyzed on immunoblots probed with indicated antibodies.

Microscopy

Cells were grown on poly-L lysine-coated glass coverslips and where indicated treated with HBSS for starvation. Cells were fixed with 4% formaldehyde for 15 min, incubated with methanol at −20°C for 10 min followed by blocking with 10% normal goat serum for 1 hr. Anti-LC3A/B antibody (Cell Signaling) was used for scoring cells undergoing autophagy. Goat-anti-rabbit Alexa Fluor 488 (Invitrogen) was used as secondary antibody. Nuclei were counterstained with Hoechst. Images were taken on a Zeiss Axio Observer Z1 microscope. For quantification, at least 50 cells were counted in three independent experiments. Statistical significance was tested using two-sided student's t test.

SUPPLEMENTAL INFORMATION

Supplemental Information includes six figures and Supplemental Experimental Procedures and can be found with this article online at doi:10.1016/j.molcel.2012.04.020.

ACKNOWLEDGMENTS

B.S. is a Leukemia and Lymphoma Society fellow, and M.B. is a Cancer Research Institute fellow. The work was supported by NCI RO1 grant CA141722 and NIGMS P50 GM085763.

Received: June 1, 2011
Revised: January 17, 2012
Accepted: April 16, 2012
Published online: May 24, 2012

REFERENCES

Amit, S., Hatzubai, A., Birman, Y., Andersen, J.S., Ben-Shushan, E., Mann, M., Ben-Neriah, Y., and Alkalay, I. (2002). Axin-mediated CKI phosphorylation of beta-catenin at Ser 45: a molecular switch for the Wnt pathway. Genes Dev. *16*, 1066–1076.

Basak, S., Kim, H., Kearns, J.D., Tergaonkar, V., O'Dea, E., Werner, S.L., Benedict, C.A., Ware, C.F., Ghosh, G., Verma, I.M., and Hoffmann, A. (2007). A fourth IkappaB protein within the NF-kappaB signaling module. Cell *128*, 369–381.

Bhattacharyya, R.P., Reményi, A., Yeh, B.J., and Lim, W.A. (2006). Domains, motifs, and scaffolds: the role of modular interactions in the evolution and wiring of cell signaling circuits. Annu. Rev. Biochem. *75*, 655–680.

Burack, W.R., and Shaw, A.S. (2000). Signal transduction: hanging on a scaffold. Curr. Opin. Cell Biol. *12*, 211–216.

Chariot, A. (2009). The NF-kappaB-independent functions of IKK subunits in immunity and cancer. Trends Cell Biol. *19*, 404–413.

Cheong, R., Bergmann, A., Werner, S.L., Regal, J., Hoffmann, A., and Levchenko, A. (2006). Transient IkappaB kinase activity mediates temporal NF-kappaB dynamics in response to a wide range of tumor necrosis factor-alpha doses. J. Biol. Chem. *281*, 2945–2950.

Comb, W.C., Cogswell, P., Sitcheran, R., and Baldwin, A.S. (2011). IKK-dependent, NF-κB-independent control of autophagic gene expression. Oncogene *30*, 1727–1732.

Courtois, G., and Israël, A. (2011). IKK regulation and human genetics. Curr. Top. Microbiol. Immunol. *349*, 73–95.

Criollo, A., Senovilla, L., Authier, H., Maiuri, M.C., Morselli, E., Vitale, I., Kepp, O., Tasdemir, E., Galluzzi, L., Shen, S., et al. (2010). The IKK complex contributes to the induction of autophagy. EMBO J. *29*, 619–631.

Dueber, J.E., Yeh, B.J., Chak, K., and Lim, W.A. (2003). Reprogramming control of an allosteric signaling switch through modular recombination. Science *301*, 1904–1908.

Dupont, N., Jiang, S., Pilli, M., Ornatowski, W., Bhattacharya, D., and Deretic, V. (2011). Autophagy-based unconventional secretory pathway for extracellular delivery of IL-1β. EMBO J. *30*, 4701–4711.

Engström, W., Ward, A., and Moorwood, K. (2010). The role of scaffold proteins in JNK signalling. Cell Prolif. *43*, 56–66.

Ferrell, J.E., Jr. (2000). What do scaffold proteins really do? Sci. STKE *2000*, pe1.

Gao, Z., Hwang, D., Bataille, F., Lefevre, M., York, D., Quon, M.J., and Ye, J. (2002). Serine phosphorylation of insulin receptor substrate 1 by inhibitor kappa B kinase complex. J. Biol. Chem. *277*, 48115–48121.

Hayden, M.S., and Ghosh, S. (2008). Shared principles in NF-kappaB signaling. Cell *132*, 344–362.

Hoffmann, A., and Baltimore, D. (2006). Circuitry of nuclear factor kappaB signaling. Immunol. Rev. *210*, 171–186.

Huang, T.T., Feinberg, S.L., Suryanarayanan, S., and Miyamoto, S. (2002). The zinc finger domain of NEMO is selectively required for NF-kappa B activation by UV radiation and topoisomerase inhibitors. Mol. Cell. Biol. *22*, 5813–5825.

Israël, A. (2010). The IKK complex, a central regulator of NF-kappaB activation. Cold Spring Harb Perspect Biol *2*, a000158.

Kim, S.Y., and Ferrell, J.E., Jr. (2007). Substrate competition as a source of ultrasensitivity in the inactivation of Wee1. Cell *128*, 1133–1145.

Lamberti, C., Lin, K.M., Yamamoto, Y., Verma, U., Verma, I.M., Byers, S., and Gaynor, R.B. (2001). Regulation of beta-catenin function by the IkappaB kinases. J. Biol. Chem. *276*, 42276–42286.

Laplantine, E., Fontan, E., Chiaravalli, J., Lopez, T., Lakisic, G., Véron, M., Agou, F., and Israël, A. (2009). NEMO specifically recognizes K63-linked poly-ubiquitin chains through a new bipartite ubiquitin-binding domain. EMBO J. *28*, 2885–2895.

Lee, D.F., Kuo, H.P., Chen, C.T., Hsu, J.M., Chou, C.K., Wei, Y., Sun, H.L., Li, L.Y., Ping, B., Huang, W.C., et al. (2007). IKK beta suppression of TSC1 links inflammation and tumor angiogenesis via the mTOR pathway. Cell *130*, 440–455.

Levchenko, A., Bruck, J., and Sternberg, P.W. (2000). Scaffold proteins may biphasically affect the levels of mitogen-activated protein kinase signaling and reduce its threshold properties. Proc. Natl. Acad. Sci. USA *97*, 5818–5823.

Makris, C., Godfrey, V.L., Krähn-Senftleben, G., Takahashi, T., Roberts, J.L., Schwarz, T., Feng, L., Johnson, R.S., and Karin, M. (2000). Female mice heterozygous for IKK gamma/NEMO deficiencies develop a dermatopathy similar to the human X-linked disorder incontinentia pigmenti. Mol. Cell *5*, 969–979.

Makris, C., Roberts, J.L., and Karin, M. (2002). The carboxyl-terminal region of IkappaB kinase gamma (IKKgamma) is required for full IKK activation. Mol. Cell. Biol. *22*, 6573–6581.

May, M.J., D'Acquisto, F., Madge, L.A., Glöckner, J., Pober, J.S., and Ghosh, S. (2000). Selective inhibition of NF-kappaB activation by a peptide that blocks the interaction of NEMO with the IkappaB kinase complex. Science *289*, 1550–1554.

Mercurio, F., Murray, B.W., Shevchenko, A., Bennett, B.L., Young, D.B., Li, J.W., Pascual, G., Motiwala, A., Zhu, H., Mann, M., and Manning, A.M. (1999). IkappaB kinase (IKK)-associated protein 1, a common component of the heterogeneous IKK complex. Mol. Cell. Biol. *19*, 1526–1538.

Nenci, A., Huth, M., Funteh, A., Schmidt-Supprian, M., Bloch, W., Metzger, D., Chambon, P., Rajewsky, K., Krieg, T., Haase, I., and Pasparakis, M. (2006). Skin lesion development in a mouse model of incontinentia pigmenti is triggered by NEMO deficiency in epidermal keratinocytes and requires TNF signaling. Hum. Mol. Genet. *15*, 531–542.

Pasparakis, M., Courtois, G., Hafner, M., Schmidt-Supprian, M., Nenci, A., Toksoy, A., Krampert, M., Goebeler, M., Gillitzer, R., Israel, A., et al. (2002). TNF-mediated inflammatory skin disease in mice with epidermis-specific deletion of IKK2. Nature *417*, 861–866.

Rudolph, D., Yeh, W.C., Wakeham, A., Rudolph, B., Nallainathan, D., Potter, J., Elia, A.J., and Mak, T.W. (2000). Severe liver degeneration and lack of NF-kappaB activation in NEMO/IKKgamma-deficient mice. Genes Dev. *14*, 854–862.

Scheidereit, C. (2006). IkappaB kinase complexes: gateways to NF-kappaB activation and transcription. Oncogene *25*, 6685–6705.

Schwartz, M.A., and Madhani, H.D. (2004). Principles of MAP kinase signaling specificity in Saccharomyces cerevisiae. Annu. Rev. Genet. *38*, 725–748.

Teo, H., Ghosh, S., Luesch, H., Ghosh, A., Wong, E.T., Malik, N., Orth, A., de Jesus, P., Perry, A.S., Oliver, J.D., et al. (2010). Telomere-independent Rap1 is an IKK adaptor and regulates NF-kappaB-dependent gene expression. Nat. Cell Biol. *12*, 758–767.

Ubersax, J.A., and Ferrell, J.E., Jr. (2007). Mechanisms of specificity in protein phosphorylation. Nat. Rev. Mol. Cell Biol. *8*, 530–541.

van Drogen, F., and Peter, M. (2002). MAP kinase cascades: scaffolding signal specificity. Curr. Biol. *12*, R53–R55.

Werner, S.L., Barken, D., and Hoffmann, A. (2005). Stimulus specificity of gene expression programs determined by temporal control of IKK activity. Science *309*, 1857–1861.

Wu, C., and Ghosh, S. (2003). Differential phosphorylation of the signal-responsive domain of I kappa B alpha and I kappa B beta by I kappa B kinases. J. Biol. Chem. *278*, 31980–31987.

Wu, D., and Pan, W. (2010). GSK3: a multifaceted kinase in Wnt signaling. Trends Biochem. Sci. *35*, 161–168.

Wu, Z.H., Wong, E.T., Shi, Y., Niu, J., Chen, Z., Miyamoto, S., and Tergaonkar, V. (2010). ATM- and NEMO-dependent ELKS ubiquitination coordinates TAK1-mediated IKK activation in response to genotoxic stress. Mol. Cell *40*, 75–86.

Xia, Y., Padre, R.C., De Mendoza, T.H., Bottero, V., Tergaonkar, V.B., and Verma, I.M. (2009). Phosphorylation of p53 by IkappaB kinase 2 promotes its degradation by beta-TrCP. Proc. Natl. Acad. Sci. USA *106*, 2629–2634.

Xu, G., Lo, Y.C., Li, Q., Napolitano, G., Wu, X., Jiang, X., Dreano, M., Karin, M., and Wu, H. (2011). Crystal structure of inhibitor of κB kinase β. Nature *472*, 325–330.

Yang, F., Yamashita, J., Tang, E., Wang, H.L., Guan, K., and Wang, C.Y. (2004). The zinc finger mutation C417R of I-kappa B kinase gamma impairs lipopolysaccharide- and TNF-mediated NF-kappa B activation through inhibiting phosphorylation of the I-kappa B kinase beta activation loop. J. Immunol. *172*, 2446–2452.